Transactions of the Japan Welding Society, Vol. 24, No. 2, October 1993

Fractography on Microcracks in Ni-base Multipass Weld Metals*

—Study on Microcracks in Multipass Weld Metals of Ni-base Alloys (Part 1)—

By Yoshikuni NAKAO*, Kenji SHINOZAKI*, Tadao OGAWA** and Hideo SAKURAI**

Abstract

Fractographic investigation on microcracks in the multipass weld metals of Ni-base alloys was carried out in order to find out the factors which caused microcracks in this study. Two types of hot cracking, viz., HAZ liquation cracking and the ductility-dip cracking were observed in the reheated zones of the multipass weld metal. According to EDX and AES analyses on microcrack surface, not only alloying elements such as Nb, Mo and Fe but also impurity elements such as P, Si and S were rich on the crack surface.

The cross-bead varestraint test was conducted in order to make clear the effects of impurity elements such as P, Si and S on the hot cracking susceptibility of the reheated weld metal of Ni-Cr-Fe ternary alloys. Base metals used were basically 70%Ni-Cr-Fe ternary alloys in which Cr contents were varied from 0 to 20%; P, Si and S contents were independently varied in the ranges of 0.002-0.032%, 0.05-1.02% and 0.001-0.02%, respectively.

Although the liquation cracking susceptibilities of all materials used were not so high, they increased with an increase in impurity elements. On the other hand, in the case of the ductility-dip cracking, the cracking susceptibilities of materials containing S were much higher than those of materials containing P and Si. Especially the cracking susceptibilities of Ni-10%Cr-20%Fe alloys were minimum among Ni-30%Fe, Ni-5% Cr-25%Fe and Ni-20%Cr-10%Fe alloys containing 0.007%S. It follows that the ductility-dip cracking susceptibility of the reheated weld metal of 70%Ni-Cr-Fe alloy strongly depended on Cr and S contents in weld metal.

Key Words: *Ni-base alloy, weld metal, multi-pass welds, microfissure, fractography, Ni-Cr-Fe ternary alloy, sulfur, phosphor, silicon, reheat cracking*

1. Introduction

It is recognized that austenitic stainless steel, nickel-base and iron-base alloy weld metals are susceptible to microcracking in multipass welds. These microcracks are too small to detect using a nondestructive testing. For this reason, it is difficult to repair them and they seem to be a quite serious problem[1,2].

Microcracking in multipass welds in austenitic stainless steels have been studied since about twenty years ago. Honeycomb[3] and Lundin[4] have reported that the mechanism of microcracking in multipass welds in austenitic stainless steels was hot cracking like liquation cracking and ductility-dip cracking. Moreover, these types of cracking have been considered to result from local melting of carbides at grain boundary and from grain boundary segregation of impurity element. However, not only characterization of microcrack but also the mechanism of microcracking in Ni-base alloy weld metal has not been made clear yet.

In this study, fractographic investigation on microcracking in overlaid welds was carried out in order to know the factors for the mechanism of microcracking. Moreover, a new testing method named the cross-bead varestraint testing was developed in order to evaluate the effect of impurity elements such as P, Si and S on the reheated weld metals of 70%Ni-Cr-Fe alloys in which Cr contents were varied from 0 to 20%.

2. Materials Used and Experimental Procedure

2.1 *Materials used*

Austenitic stainless steel, SUS304 (20mm^t) and 9%Ni steel (25mm^t) were used for the base plate. The overlaid weld metals were deposited on these base plates by commercial electrodes such as ENiCrFe-1(E1) and ENiCrMo-3(E2) and a tentative electrode, Ni-Mo type(E3) rod using SMA welding and then cross-sections of multipass welds were observed to reveal microcracks. The chemical compositions of these materials are listed in Table 1.

In order to evaluate the effects of the impurity elements on hot cracking susceptibility in Ni-Cr-Fe ternary alloys, four kinds of base metals such as Ni-30%Fe (0Cr alloy), Ni-5%Cr-25%Fe (5Cr alloy), Ni-10%Cr-20%Fe (10Cr alloy) and Ni-20%Cr-10%Fe (20Cr alloy) varying in the contents of P, S and Si were used. The hot cracking susceptibilities of the reheat-

* Received: 29 July, 1993

** Member, Faculty of Engineering, Osaka University: 2-1 Yamada-oka, Suita, Osaka 565 JAPAN

*** Member, Nippon Steel Corp. 20-1 Shintomi, Futtsu, Chiba 299-12 JAPAN

Table 1 Chemical compositions of base metals and deposited metals used for the overlaid weld test.

		Chemical composition (mass%)											
		C	Si	Mn	P	S	Ni	Cr	Fe	Mo	W	Nb+Ta	O
Base metal	SUS304	0.04	0.23	0.55	0.008	0.007	8.76	-	Bal.	-	-	-	-
	9%Ni steel	0.06	0.42	0.88	0.034	0.002	8.35	18.11	Bal.	-	-	-	-
Electrode	E-1	0.056	0.28	0.5	0.009	0.008	59.7	22.1	4.7	9.0	-	3.3	-
	E-2	0.05	0.27	2.95	0.002	0.003	71.06	14.32	8.98	-	-	2.03	-
	E-3	0.05	0.21	1.64	0.004	0.004	72.4	-	3.88	18.9	3.16	-	0.0206

Table 2 Chemical compositions of 70%Ni-Cr-Fe ternary alloys used for the cross-bead varestraint test.

Alloy	Heat No.	Chemical compositions (mass%)									
		C	Mn	Si	P	S	Cr	Fe	Mo	N	Ni
Ni-30Fe	F-B	0.015	0.330	0.05	0.002	0.001	0.110	32.16	0.01	0.0004	Bal.
	F-Si1	0.016	0.300	0.44	0.002	0.001	0.16	31.38	0.01	0.0004	Bal.
	F-Si2	0.018	0.34	1.02	0.003	0.0018	-	30.2	-	0.0005	Bal.
	F-P1	0.013	0.30	0.047	0.022	0.0021	-	31.1	-	0.005	Bal.
	F-P2	0.012	0.30	0.05	0.032	0.0021	-	30.0	-	0.0005	Bal.
	F-S1	0.015	0.30	0.044	0.003	0.007	-	30.2	-	0.0005	Bal.
	F-S2	0.014	0.30	0.05	0.002	0.021	-	30.0	-	0.005	Bal.
Ni-5Cr-25Fe	5CF-B	0.013	0.29	0.05	0.002	0.001	4.86	25.48	0.10	0.0005	Bal.
	5CF-Si1	0.018	0.29	0.41	0.002	0.001	4.69	25.28	0.04	0.0006	Bal.
	5CF-Si2	0.016	0.32	1.02	0.004	0.0015	4.71	25.2	-	0.0007	Bal.
	5CF-P1	0.017	0.30	0.05	0.021	0.001	4.65	27.01	0.01	0.0006	Bal.
	5CF-P2	0.017	0.34	0.053	0.032	0.0004	4.82	25.5	-	0.0008	Bal.
	5CF-S1	0.015	0.32	0.04	0.002	0.0075	4.77	25.6	0.01	0.0006	Bal.
	5CF-S2	0.015	0.30	0.046	0.003	0.020	5.09	24.9	-	0.001	Bal.
Ni-10Cr-20Fe	10CF-B	0.017	0.29	0.052	0.003	0.0012	9.98	20.1	-	0.0006	Bal.
	10CF-Si1	0.016	0.33	0.37	0.003	0.0003	9.61	20.8	-	0.0006	Bal.
	10CF-Si2	0.017	0.33	1.01	0.002	0.001	9.53	20.0	-	0.005	Bal.
	10CF-P1	0.017	0.3	0.05	0.021	0.001	10.0	20.0	-	0.005	Bal.
	10CF-P2	0.016	0.34	0.052	0.045	0.0004	9.65	19.3	-	0.0007	Bal.
	10CF-S1	0.016	0.30	0.046	0.003	0.007	10.05	20.5	-	0.0006	Bal.
	10CF-S2	0.014	0.30	0.05	0.002	0.021	10.0	20.0	-	0.005	Bal.
Ni-20Cr-10Fe	20CF-B	0.021	0.31	0.04	0.002	0.0015	20.75	9.82	0.01	0.0014	Bal.
	20CF-Si1	0.02	0.32	0.40	0.002	0.001	20.44	10.04	0.02	0.0018	Bal.
	20CF-Si2	0.016	0.36	0.99	0.003	0.0003	19.87	9.4	-	0.0014	Bal.
	20CF-P1	0.018	0.30	0.04	0.021	0.0017	19.82	9.44	0.17	0.002	Bal.
	20CF-P2	0.028	0.35	0.1	0.042	0.0010	19.59	10.05	-	0.0012	Bal.
	20CF-S1	0.017	0,27	0.052	0.003	0.007	20.17	13.6	-	0.0008	Bal.
	20CF-S2	0.016	0.30	0.05	0.002	0.019	20 0	10.0	-	0.005	Bal.

ed weld metals of them were evaluated using the cross-bead varestraint testing. The chemical compositions of Ni-Cr-Fe ternary alloys are listed in Table 2.

2.2 *Overlaid weld test*

The specimens were assembled both by building up three layers with 4-5 weld beads each on SUS304 stainless steel plate using the electrodes, E1 and E2 and by building up four layers with 5-6 beads each on 9% Ni steel plate using the electrode, E3 as shown in Fig. 1. The welding parameters such as welding current, arc voltage and travel speed were 130A, 22V and 4.2 mm/s using electrodes, E1 and E2, and 170A, 26V and 2.8 mm/s using an electrode, E3, respectively. The weld bead sequence was deposited at a temperature range below 323K. Microcracks (magnified 400 times) were determined in the cross-section of weld beads divided in the long direction at intervals of 10 mm using an optical microscope.

2.3 *The cross-bead varestraint testing*

The cross-bead varestraint test was developed in order to evaluate the hot cracking susceptibilities in the reheated weld metals. Figure 2 shows the cross-bead varestraint testing. Firstly a weld bead named the first bead was laid by GTA welding with the welding parameters of 100A, 14V and 0.83 mm/s. Secondly the cross-bead, which was perpendicular to the first bead, was laid from the point, A in Fig. 2 and when the molten pool of a cross-bead came just into the first bead the specimen was bent instantly and at the same time the arc was turned off immediately. Subsequently cracks occurred in the HAZ of the first bead.

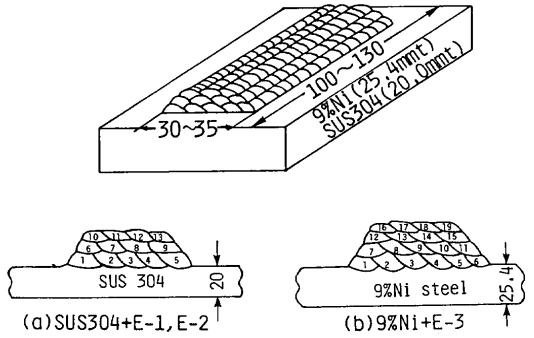

Fig. 1 The overlaid weld test.
(a) SUS304+E1, E2 (b) 9%Ni steel+E3

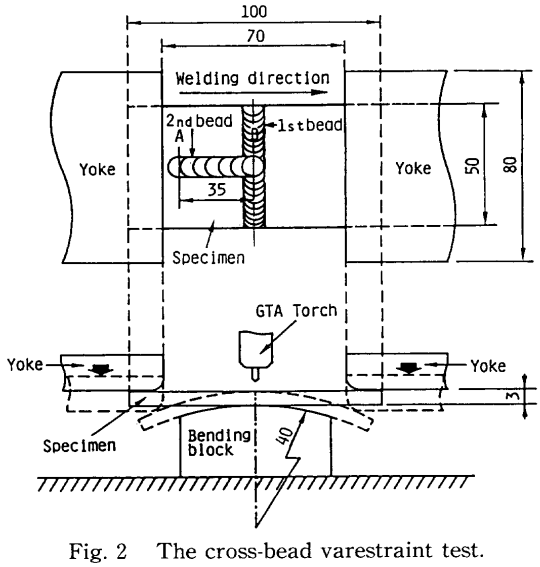

Fig. 2 The cross-bead varestraint test.

The augmented strain was 4.2%. The welding parameters of the cross-bead were 100A, 14V and 1.67 mm/s. Cracks (magnified 20 to 40 times) were determined using an optical microscope.

3. Characteristics of Microcracks in Multipass Welds

3.1 *Microcrack appearance and location*

Total number of microcracks in all specimens examined were 24. All microcracks examined in this investigation, regardless of weld metal type, were located in the HAZ of a subsequently deposited bead. Based on the relation between interpass boundary and crack location, crack location was classified in three different types such as Types I, II and III. That is, in Fig. 3, light micrographs showing cracks in a polished and etched cross-section of weld pad, indicate that the crack occurs away from the interpass boundary (Type I) (see Fig. 3(a)), that the crack is adjacent to the interpass boundary (Type II) (see Fig. 3(b)) and that the crack crosses the interpass boundary (Type III) (see Fig. 3(c)), respectively. Most of crack lengths are less than 0.5mm as shown in Fig. 4. 70% of total cracks are Type I, so that Type I crack seems to occur easily. Such a crack is located along γ phase grain boundary as shown in Fig. 5 regardless of weld metal type.

3.2 *Crack surface morphology*

To gain insight into the mechanism of crack formation, the surfaces of the microcracks in weld metal types were examined utilizing the scanning electron microscope. Figure 6(a) shows the macroscopic surface morphology of Type III crack (No. 21). Figure 6(b), (c) and (d) show the enlarged surface morphologies at the positions of A, B and C in Fig. 6(a). This feature suggests, as has been shown by Weise[5], that a liquid film existed in this region when separation of the material occurred causing a crack, so that this type of crack was regarded as a liquation crack. This characteristic surface was defined as Mode I. Figure 7(a) shows the macroscopic surface morphology of Type I crack (No. 14) located at a distance of 1.3mm from the interpass boundary. Figure 7(b) and (c) show the enlarged microstructures at positions of A and B in Fig. 7(a). These fracture surface morphologies are different from those surfaces typified in Figs. 6(b), (c) and (d). Although the surfaces are relatively smooth and somewhat finer, there is no characteristic prior presence of liquid film observed. Therefore this type crack seems to be a ductility-dip cracking. This characteristic surface was defined as Mode II. The modes of other crack surface morphologies examined belon-

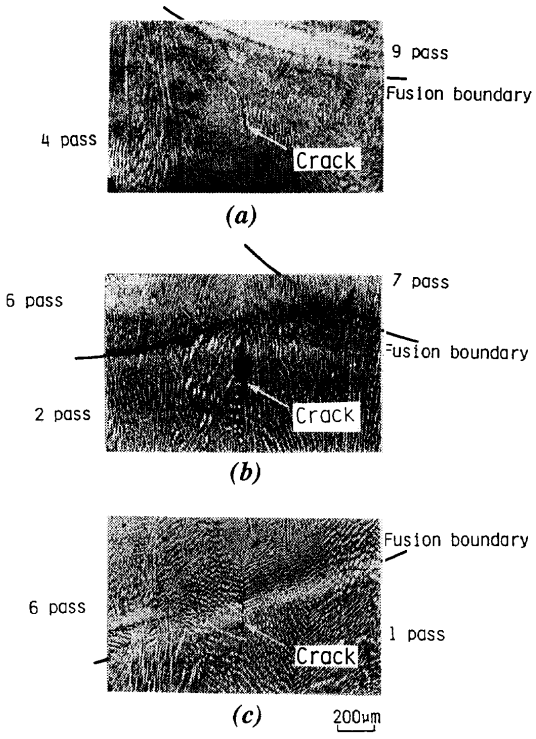

Fig. 3 Microcrack appearance and location in the multipass welds.
(a) Type I (b) Type II (c) Type III

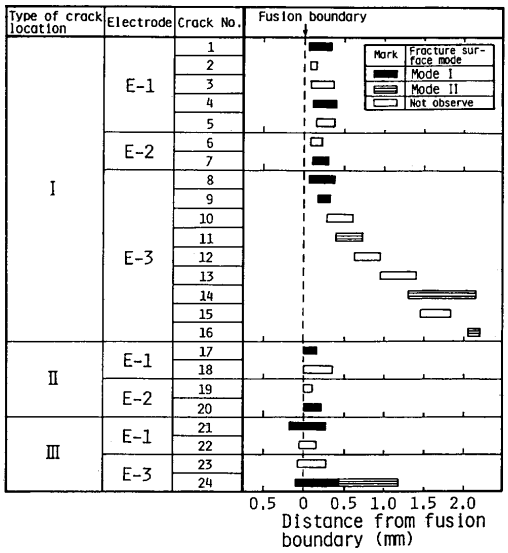

Fig. 4 Relation between fusion boundary and both location and fracture modes of all microcracks.

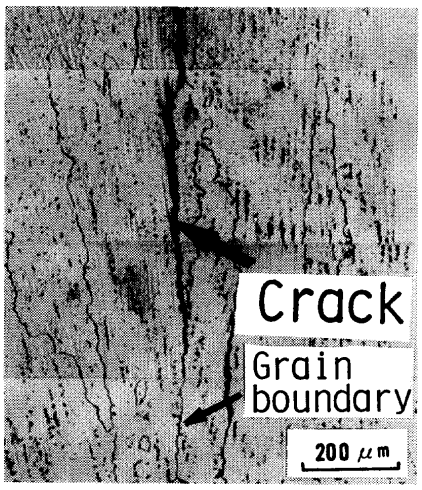

Fig. 5 Microcracks occurring along γ phase grain boundary in multipass welds.

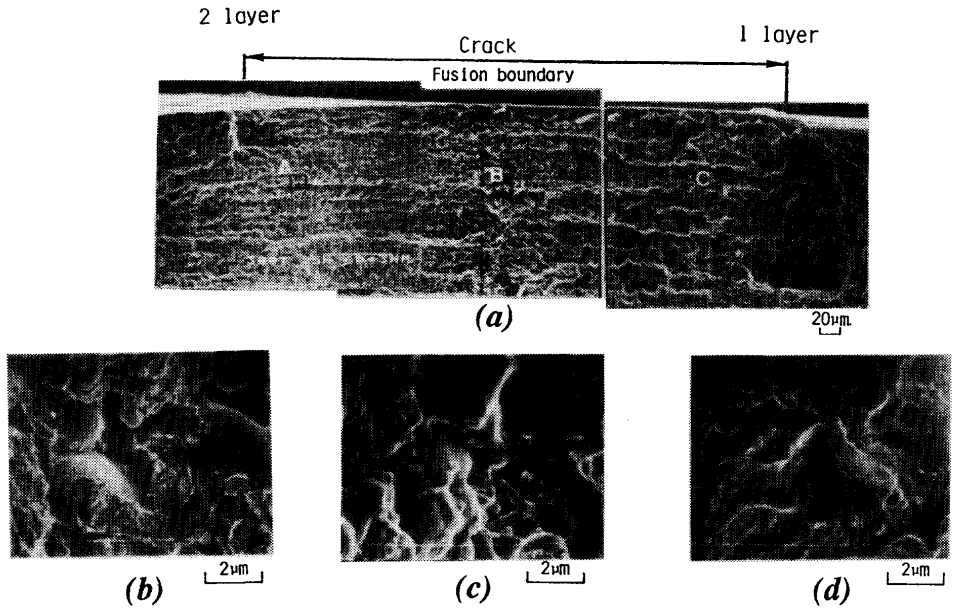

Fig. 6 SEM microstructures of microcracks in the multipass welds (crack No.: No.21). (a) general appearance of crack surface, (b) enlarged surface at A, (c) enlarged surface at B, (d) enlarged surface at C.

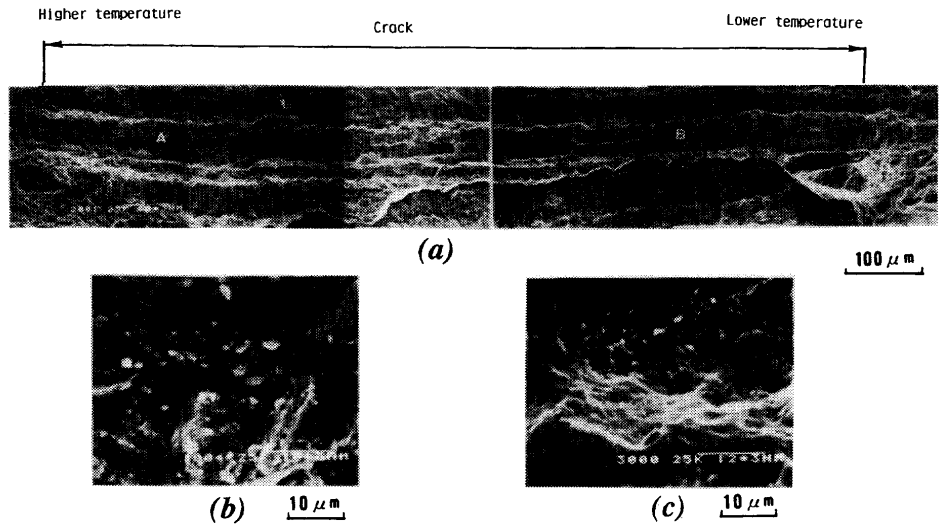

Fig. 7 SEM microstructures of microcracks in the multipass welds (crack No.: No.14). (a) general appearance of crack surface, (b) enlarged surface at A, (c) enlarged surface at B

ged to Mode I or II regardless of types of cracks. Figure 4 also shows the mode of fracture surface morphologies of each crack. It is apparent that Mode I appeared in the cracks occurring within about 0.5 mm from the interpass boundary and Mode II did in the cracks occurring more than about 0.5mm away from the interpass boundary. Thus, it can be concluded that microcracks occur in the weld metal HAZs produced by subsequent weld passes and both HAZ liquation and ductility-dip cracking occur in the weld metal at the same time. HAZ liquation cracking in the weld metal is more prone to occur than ductility-dip cracking.

3.3 *Energy dispersive analysis*

To make clear the mechanism of both liquation and ductility-dip cracking, both energy dispersive X-ray analysis on the crack surface and X-ray diffraction of extracted residue from the weld metal were performed in an attempt to document segregation of certain elemental species. Table 3 summarizes identifications of microconstituents on the crack surface of each weld metal. Since the phases such as NbC, Fe_2(Nb, Mo) and Mo_2C were observed on the crack surfaces, it is apparent that the crack surfaces are enriched with Nb, Fe and Mo.

3.4 *Auger electron analysis*

It has been reported by many investigators that certain harmful elements such as Si, P and S caused hot cracking. Energy dispersive X-ray analysis doesn't have the capability of detecting, even qualitatively, small amounts of trace elements on fracture surfaces. Auger electron spectroscopy is perhaps an alternative

Table 3 Summary of EDX analyses and identifications of microconstituents on crack surface of weld metals using electrodes, E1, E2 and E3.

Electrode	Constituent element of precipitates on fracture surface by EDX	Phase
E-1	Nb, Mo	NbC, Fe_2(Nb, Mo)
E-2	Nb	NbC
E-3	Mo	Mo_2C

approach to the problem although it is difficult to apply.

Figure 8 shows the relative peak heights of P, Si and S to Mo and Ni on the crack surface and artificially fractured intragranular surface of weld metals using electrodes, E1 and E3. As it was difficult to identify the peak of P from Mo at the same electron energy of 120eV and also the peak of S at an electron energy of 152eV from Mo at 148eV, combined peak heights, (Mo+P) and (Mo+S) were used in this figure. Comparing the relative peak heights of P, Si and S on liquation and ductility-dip crack surfaces with intragranular fractured surfaces, the former is higher than the latter regardless of the type of cracking. Thus, it is apparent from Fig.8 that harmful elements such as P, Si and S segregate at the γ phase grain boundary.

4. Hot Cracking Susceptibility in the Reheated Weld Metal

Certain harmful impurity elements such as P, Si and S may cause the microcracks. The cross-bead varestraint testing was conducted in the reheated weld metal passes of 70%Ni-Cr-Fe ternary alloys containing P, Si and S in which Cr contents were varied from 0 to 20% in an attempt to document the effect of impurity elements on hot cracking susceptibility of the reheated weld metal.

From the standpoint of location of crack, two types of cracks occurred in the reheated weld metal in the cross-bead varestraint test regardless of weld metal. That is, the crack is adjacent to the fusion boundary, being located at a distance of about 0.5mm from the fusion boundary as shown in Fig. 9(a) and (b). Both cracks are located along weld metal grain boundaries in the HAZ of the first bead.

Based on the morphologies of the crack surfaces, the cracks as shown in Fig. 9(a) and (b) are regarded as a liquation crack and a ductility-dip crack, respectively. In addition, these crack surface morphologies are quite similar to those in Figs. 6 and 7. Thus, it is concluded that microcracks occurring in the multipass weld metal are reproduced by the cross-bead varestraint testing.

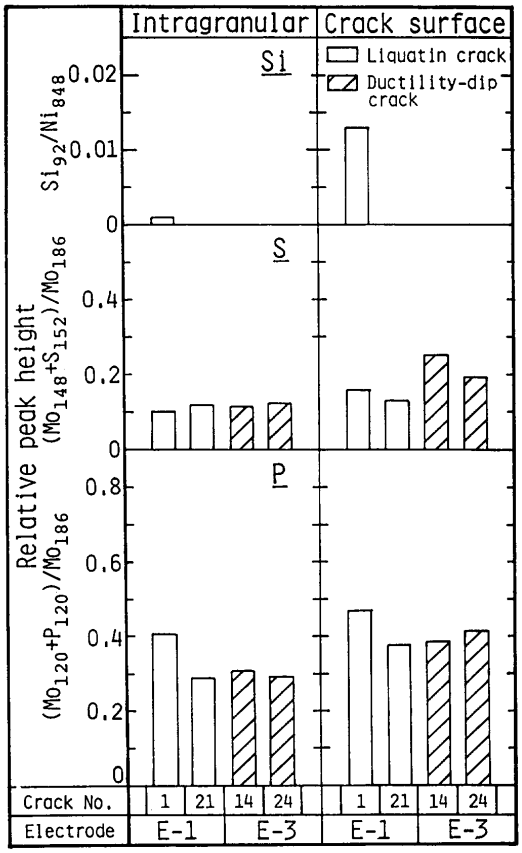

Fig. 8 Comparison of P, S and Si contents on intergranular surface with those on intragranular fracture surface of microcracks analyzed by AES.

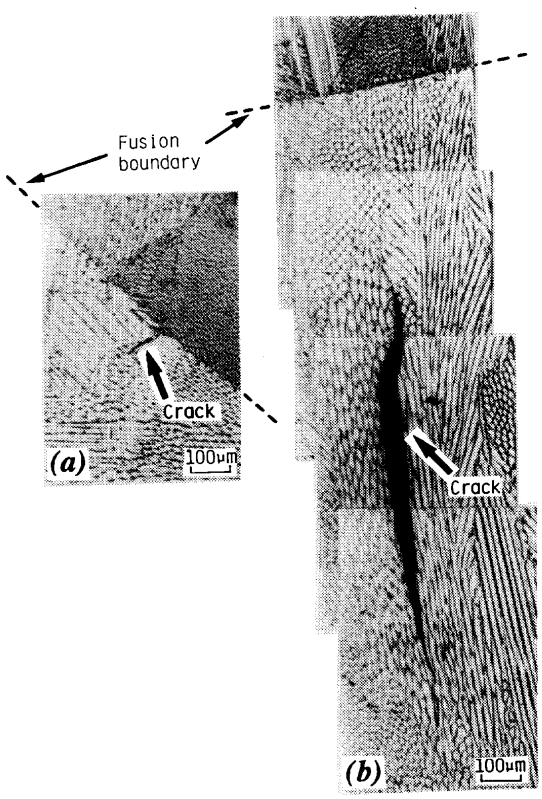

Fig. 9 Hot cracking in the reheated weld metals obtained by the cross-bead varestraint test.
(a) HAZ liquation crack, (b) ductility-dip crack

4.1 *HAZ liquation cracking susceptibility*

HAZ liquation cracking susceptibilities in the reheated weld metals were evaluated using a maximum crack length. Figure 10 shows the maximum crack length covering the different P, S and Si contents varying Cr contents from 0 to 20% of weld metals. The HAZ liquation cracking susceptibilities of the reheated weld metals of these materials generally seem to be low because the values of the maximum crack length of are not so high regardless of high amount of impurity elements and high augmented strain. However, this result shows that the HAZ liquation cracking susceptibility of the reheated weld metal increases with an increase in the impurity elements such as P, Si and S regardless of Cr contents. As a solidification crack occurred in the first bead containing about 0.021%S, the cross-bead varestraint testing wasn't conducted in this weld metal.

4.2 *Ductility-dip cracking susceptibility*

Ductility-dip cracking susceptibilities were evaluated with the total number of cracks. Figure 11 shows the total number of ductility-dip cracks covering the different P, S and Si contents varying Cr contents from 0 to 20% of weld metals. It should be pointed out that although the effects of P and Si on the cracking susceptibilities are not clear, S strongly affects the cracking susceptibility, viz., an increasing S content increases the cracking susceptibility. In addition, the ductility-dip cracking susceptibilities of the weld metals strongly depend on Cr content, viz., cracking susceptibility of 10Cr alloy containing 0.007%S is minimum among 0Cr, 5Cr and 20Cr alloys.

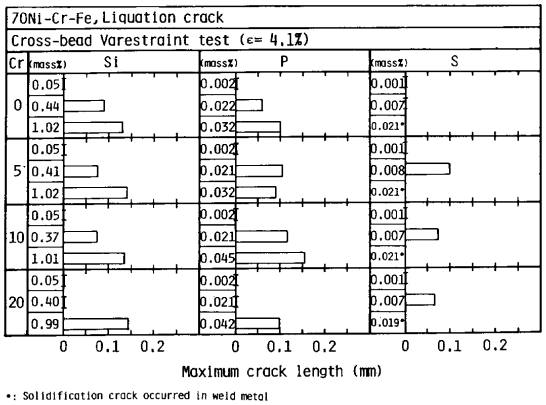

Fig. 10 Effects of P, Si and S contents on maximum crack length of liquation cracking in the reheated weld metals of 70%Ni-Cr-Fe ternary alloys.

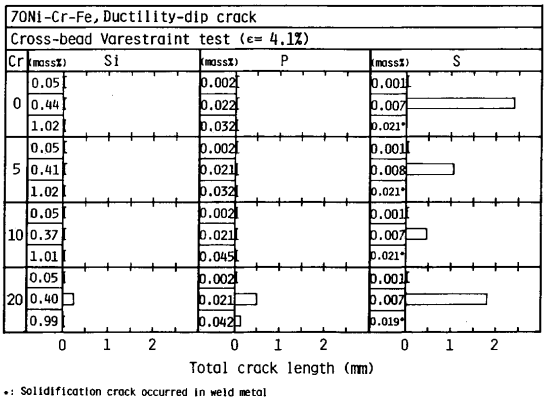

Fig. 11 Effects of P, Si and S contents on total crack length of ductility-dip cracking in the reheated weld metals of 70%Ni-Cr-Fe ternary alloys.

It can be concluded that an increasing P and Si increases the liquation cracking susceptibilities of the weld metals and an increasing S increases the liquation and the ductility-dip cracking susceptibilities. In addition, especially the ductility-dip cracking susceptibility of weld metals strongly depends on Cr and S contents in the weld metals of 70%Ni-Cr-Fe ternary alloys.

5. Conclusions

In this study, fractographic investigation for microcracks in the overlaid welds was carried out in order to gain insight into the mechanism of microcracking in the Ni-base multipass welds. Moreover, a new testing method named the cross-bead varestraint testing was developed in order to evaluate the effect of the impurity elements such as P, Si and S on the reheated weld metals of 70%Ni-Cr-Fe alloys in which Cr contents were varied from 0 to 20%. The following results and conclusions were obtained:

(1) The microcracks occurring in the overlaid multipass welds were located along γ phase grain boundary and most of the crack lengths were within about 0.5mm.

(2) According to examination of microcrack surfaces, the HAZ liquation cracking was adjacent to the interpass boundary and the ductility-dip cracking was located at a distance of more than 0.5mm from the interpass boundary. These crackings were prone to form in the weld metal HAZs produced by subsequent weld passes.

(3) The phases such as NbC, Fe_2(Nb, Mo) and Mo_2C were observed on the crack surfaces. This meant that the crack surfaces were enriched with the alloying elements such as Nb, Mo and Fe.

(4) According to the auger electron analysis on the crack surfaces, the impurity elements such as P, Si and S were also rich on the crack surfaces.

(5) The newly developed cross-bead varestraint test technique for the reheated weld metal was able to reproduce the weld metal HAZ liquation and ductility-dip cracking in the multipass welds.

(6) According to the cross-bead varestraint test of 70%Ni-Cr-Fe ternary alloys containing P, S and Si in which Cr contents were varied from 0 to 20%, the HAZ liquation cracking susceptibility of the reheated weld metal increased with an increase in the impurity elements such as P, Si and S regardless of Cr contents. On the other hand, S strongly affected the ductility-dip cracking susceptibility, viz. an increasing S content increased the cracking susceptibility. In addition, the ductility-dip cracking susceptibilities of the weld metals strongly depended on Cr content, viz., cracking susceptibility of 10Cr alloy containing 0.007%S was

minimum among 0Cr, 5Cr and 20Cr alloys.

Acknowledgement

The authors wish to thank their students, especially Mr.Y. Tamura at Osaka University for his help.

References

1) J. N. Cordea, P. A. Kammer and D. C. Martin: Cause of Fissuring in Nickel-Base and Stainless Alloy Weld Metals, Welding J., 43 (1964) 9, p.481s
2) N. Morishige and H. Okabayashi: Microcracking in Weld Metals of Nickel Alloys and Austenitic Stainless Steels (Report 1), J. JWS, 51 (1982) 12, p.40 (in Japanese)
3) J. Honeycomb and T.G. Gooch: Microcracking in Fully Austenitic Stainless Steel Weld Metal, Metal. Const. & British Weld. J., 2 (1970) 9, p.375
4) C. D. Lundin and C. P. D. Chou: Fissuring in the "Hazard HAZ" Region of Austenitic Stainless Welds, Welding J., 64 (1985) 4, p.113s
5) B. Weise, G. E. Grotke and R. Stickler: Physical Metallurgy of Hot Ductility Testing, Welding J., 49 (1970) 10, p. 471s